https://doi.org/10.5194/egusphere-2023-1047
Preprint. Discussion started: 19 June 2023

Nitrous oxide emissions from pan-Arctic terrestrial ecosystems: A process-based biogeochemistry model analysis from 1969 to 2019

Ye Yuan[1], Qianlai Zhuang[1], Bailu Zhao[1], and Narasinha Shurpali[2]

[1]Earth, atmospheric, and planetary science department, Purdue University, West Lafayette IN 47906

[2]Natural Resources Institute Finland (Luke), Latokartanonkaari 9, FI-00790 HELSINKI, FINLAND

Correspondence to: qzhuang@purdue.edu

Abstract: Nitrous oxide (N_2O) is a potent greenhouse gas with radiative forcing 265-298 times stronger than that of carbon dioxide (CO_2). Increasing atmospheric N_2O burden also contributes to stratospheric ozone depletion. Recent field studies show N_2O emissions from the Arctic ecosystems have increased due to warming. To date, the emissions across space and time have not been adequately quantified. Here we revised an extant process-based biogeochemistry model, the Terrestrial Ecosystem Model (TEM) to incorporate more detailed processes of soil biogeochemical nitrogen (N) cycle, permafrost thawing effects, and atmospheric N_2O uptake in soils. The model is then used to analyze N_2O emissions from pan-Arctic terrestrial ecosystems. We find that both regional N_2O production and net emissions increased from 1969 to 2019, with production ranging from 1.2 - 1.3 Tg N yr $^{-1}$ and net emissions from 1.1 - 1.2 Tg N yr^{-1} considering the permafrost thaw effects. Soil N_2O uptake from the atmosphere was 0.1 Tg N yr $^{-1}$ with a small interannual variability. Atmospheric N deposition significantly increased N_2O emission by 31.5 ± 3.1%. Spatially, terrestrial ecosystems act as net sources or sinks ranging

https://doi.org/10.5194/egusphere-2023-1047
Preprint. Discussion started: 19 June 2023

from -12 to 700 mg N m^{-2} yr^{-1} depending on temperature, precipitation, soil characteristics, and vegetation types in the region.

1. Introduction

Global climate change entails rising temperatures, a change in precipitation patterns, and a more frequent occurrence of extreme weather events. The common consensus is that temperature increase will be most pronounced in the northern high latitudes (Overland et al., 2013). Pan-Arctic land areas are predicted to warm up to 5.6–12.4 °C by the end of this century (IPCC, 2013), leading to widespread permafrost degradation and thaw (Borge et al., 2017; Jones et al., 2016; Romanovsky et al., 2010) and substantial changes in ecosystem functioning (Grosse et al., 2016), accelerating decomposition of permafrost soil organic matter (SOM) and stimulating greenhouse gas (GHG) emissions (Yang et al., 2010; Sierra et al., 2015; Voigt et al., 2017). Permafrost soils are also large nitrogen (N) reservoirs (Post et al., 1985), with a conservative estimate of 67 billion tons of total N in the upper 3 m (Harden et al., 2012). The storage of organic nitrogen supplies plenty of substrates for nitrification and denitrification.

While past studies on greenhouse gas emissions from the Arctic have mainly focused on carbon-based compounds, recent studies show that Arctic soils might also be a significant source of N_2O from peatlands (Repo et al., 2009; Marushchak et al., 2011), and high N_2O production potential in soils after permafrost thaw (Elberling et al., 2010). Elevated soil N_2O concentrations have been observed in upland tundra due to thawing permafrost (Abbott & Jones, 2015). Furthermore, rising temperatures also promote N_2O emissions from tundra ecosystems (Vigot et al., 2017), which cover large areas of the Arctic. The great unknown, however, is how permafrost thaw affects N_2O emissions by potentially unlocking the vast N stocks currently stored in Arctic soils (Harden et al., 2012). Although Arctic N_2O fluxes are low on a mass basis,

https://doi.org/10.5194/egusphere-2023-1047
Preprint. Discussion started: 19 June 2023

they are important since N_2O is a more potent GHG with radiative forcing of 265-298 times stronger than that of CO_2 (IPCC, 2013). N_2O contributes nearly 10% of the total anthropogenic radiative forcing and is among the key chemicals destroying the stratospheric ozone layer (Ravishankara et al., 2009).

Soil temperature, moisture, acidity, soil organic matter (SOM) content, C/N ratio, and plant growth have been identified as the key regulators of Arctic N_2O emissions (Marushchak et al., 2011; Voigt et al., 2017; Smith et al. 1998). Soil temperature involves in both organic and inorganic processes in the N cycle. Soil moisture determines the rates of gas destruction via oxidation. High water content leads to the low oxygen condition, which is associated with reducing environment, whereas less water leads to an oxidizing environment. Soil acidity controls the chemical reactions involving H^+ or OH^-, both of which influence the activity of microorganisms and enzymes (Kunhikrishnan et al., 2016). Traditionally, N_2O emissions originating from areas of high latitudes are viewed as an insignificant source (Martikainen et al. 1993, Potter et al. 1996) due to a slow mineralization rate under low temperature, humid conditions, and low atmospheric deposition of nitrogen (Dentener et al. 2006). In pan-Arctic terrestrial ecosystems, the shortage of mineral N used to be one of the main reasons for the low nitrous oxide (N_2O) emissions measured from tundra soils (Ludwig et al., 2006; Ma et al., 2007). However, in recent decades, the warming climate and loss of permafrost may disrupt the past closed Arctic N cycling and cause significant export of inorganic N (Frey et al. 2007; McClelland et al. 2007). Such patterns may result from the introduction of previously frozen N into the cycling pool due to gradual degradation of permafrost that deepens the zone of seasonally thawed soils, or from direct effects of temperature on microbial processes.

https://doi.org/10.5194/egusphere-2023-1047
Preprint. Discussion started: 19 June 2023

To date, a group of process-based biogeochemistry models have been used to quantify N_2O fluxes, including a version of Terrestrial Ecosystem Model (TEM) (Qin et al. 2014,2015; Yu, 2016; Yu and Zhuang 2019), the Community Land Model, Carbon and Nitrogen cycles (CLM-CN) (Saikawa et al. 2013), the daily Century (DayCent) model (Parton et al. 1998, Del Grosso et al. 2005), and the Denitrification/ Decomposition (DNDC) Model (Li 1992). However, none of them has included the Arctic permafrost thawing effects on N_2O emission and N_2O uptake from atmosphere in modeling. Here we further develop the TEM based on the version of the model in Yu (2016) and Yu and Zhuang (2019) by incorporating the effects of permafrost thawing on nitrogen mineralization and the soil N_2O uptake from the atmosphere. The model is then parameterized and verified and applied to quantify N_2O emissions from pan-Arctic terrestrial ecosystems from 1969 to 2019.

2 Method

2.1 Model Description

TEM is a global-scale biogeochemical model designed to quantify the cycling of carbon (C) and nitrogen (N) in terrestrial ecosystems (Melillo et al., 1993; Zhuang et al., 2003; Yu, 2016; Yu and Zhuang., 2019). The major processes of nitrogen (N) dynamic module were inherited from Yu and Zhuang (2019), including the effect of physical conditions on both nitrification and denitrification, as well as the principles of the stoichiometry of carbon and nitrogen dynamics in soils. Here we revised the N cycling algorithms in TEM by incorporating the loss of nitrogen through gas emissions, the uptake of N_2O from the atmosphere, and additional inputs of organic nitrogen and carbon resulting from permafrost thawing (Fig. 1).

https://doi.org/10.5194/egusphere-2023-1047
Preprint. Discussion started: 19 June 2023

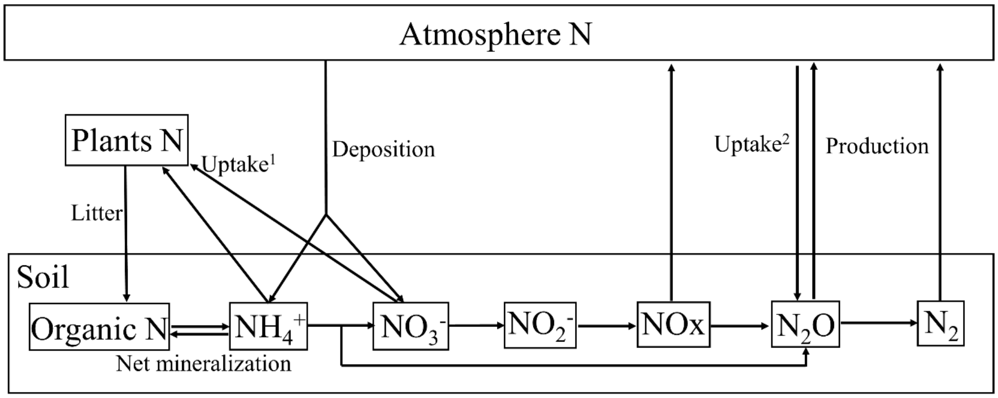

Figure 1. Nitrogen cycle and N_2O production in the revised Terrestrial Ecosystem Model. Net mineralization: the difference between mineralization (organic N mineralized to inorganic N) and mobilization (inorganic N to organic N); Litter: organic N from plant litters; Uptake[1]: inorganic N uptake by plants; Deposition: Atmospheric deposition of N; Production: N_2O production in soils; Uptake[2]: atmospheric N_2O uptake in soils.

The net N_2O emission is calculated as the difference between N_2O production (N_P) in soils and soil N_2O uptake (N_U) from the atmosphere. We include N_2O generated from nitrification (N_N) and denitrification (N_{DN}) in the total N_2O production:

$$N_E = N_P - N_U \quad (1)$$

$$N_P = N_N + N_{DN} \quad (2)$$

The amount of N_2O uptake is calculated according to Fick's law of gas diffusion (Eq. 3), where C_{air} and C_{soil} represent N_2O concentration in air and soils, respectively.

$$N_U = (C_{air} - C_{soil}) \times k_S \quad (3)$$

We use atmospheric N_2O concentrations of 331.1 ppb. k_S represents the diffusion coefficient. The N_2O diffusion coefficient used in this study is 1.26×10^{-6} m^2 s^{-1} (van Bochove, Bertran, & Caron, 1998).

The N_P from nitrification was determined by a fraction of the nitrification rate k_n, which

https://doi.org/10.5194/egusphere-2023-1047
Preprint. Discussion started: 19 June 2023

is 0.02 in the DayCent model (William et al. 1998, Delgrosso et al. 2005), and 0.0006 in the DNDC Model (Li 1992). In this study, we varied k_n within the range of 0.0006 to 0.02 and calibrated it using observational data. The NI_P from denitrification, k_{dn}, is the fraction of denitrified N lost as N_2O fluxes, calculated based on the ratio of N_2 to the sum of N_2 and N_2O ($N_2/(N_2+N_2O)$) from denitrification, which is influenced by soil moisture, pH and electron level. The effects of electron donor to the substrate (f_{nc}) and water function to N_2 ratio (f_m) are from Del Grosso et al (2000), in which the pH function for N_2/N_2O ratio ($f_{ph_{rn2}}$) is derived from the SWAT model (Wagena et al, 2017):

$$N_N = k_n \times f_{nit} \quad (4)$$

$$N_{DN} = k_{dn} \times f_{deni} \quad (5)$$

$$k_{dn} = \frac{1}{1+r_{n2}} \quad (6)$$

$$r_{n2} = f_{nc} \times f_m \times f_{ph_{rn2}} \quad (7)$$

$$f_{ph_{rn2}} = \begin{cases} 0.1, & (pH \leq 4.5) \\ \frac{1}{1470 \times e^{-1.1 \times pH}}, & (pH > 4.5) \end{cases} \quad (8)$$

$$f_{nc} = \begin{cases} k_1 \times e^{(-0.8 \times \frac{no3}{co2})}, & (0.16 \times k_1 \leq k_1 \times e^{(-0.8 \times \frac{no3}{co2})}) \\ 0.16 \times k_1, & (0.16 \times k_1 > k_1 \times e^{(-0.8 \times \frac{no3}{co2})}) \end{cases} \quad (9)$$

$$k_1 = \begin{cases} 1.7, & ((38.4 - 350 \times \text{diff}) < 1.7) \\ 38.4 - 350 \times \text{diff}, & ((38.4 - 350 \times \text{diff}) \geq 1.7) \end{cases} \quad (10)$$

$$f_m = \begin{cases} 0.1, & ((0.015 \times \text{wfps} - 0.32 < 0.1) \\ 0.015 \times \text{wfps} - 0.32, & ((0.015 \times \text{wfps} - 0.32 \geq 0.1) \end{cases} \quad (11)$$

To assess the impact of permafrost thaw on N mineralization, we account for the additional nitrogen and carbon input due to permafrost thaw depth changes. The thawing depth in the current year was compared with the maximum thawing depth in previous years. If the

https://doi.org/10.5194/egusphere-2023-1047
Preprint. Discussion started: 19 June 2023

thawing depth in the current year exceeded the maximum thawing depth in past years, the thawing depth difference was considered as the thawing depth change, and the organic N and C between two depths were added to soil organic N and C pools. We based our calculation on a soil thermal model, detailed information can be found in Liu et al. (2022) and Zhuang et al. (2001). Due to lacking permafrost deep layer profile data of C and N, we assumed they are uniformly distributed in vertical (Wang et al., 2020), with nitrogen density of 2 kg m^{-3} (Strauss et al., 2022) and C density of 29 kg m^{-3} (Mishra et al., 2021), and half of the total N and C (1 kg m^{-3} and 14.5 kg m^{-3}) are organic that will undergo N mineralization and release.

2.2 Model parameterization and verification

We conducted model parameterization using observation data from 22 sites across the pan-Arctic region, including 4 wet tundra sites, 12 boreal forest sites, and 6 alpine tundra sites (Table.1).

Table 1: Site description for N_2O emission observations that are used for model parameterization and verification.

Site	**Classification**	**Location**	**Country**	**Latitude**	**Longitude**	**Soil bulk density (g cm^{-3})**	**pH**	**Time**	**Reference**
W1	Wet Tundra	Inner Mongolia	China	N 49.3	E 119.9	1.2	4.9	2008-5 to 2009-9	Liu et al (2017)
W2	Wet Tundra	Yakutsk, eastern Siberia	Russia	N 62.5	E 129.5	1.0	8.0	2004-6 to 2005-9	Takakai et al. (2008)
W3	Wet Tundra	Seida	Russia	N 67	E 63	0.0	3.7	2012-07 to	Voigt et al. (2017)

https://doi.org/10.5194/egusphere-2023-1047
Preprint. Discussion started: 19 June 2023

								2013-09	
W4	Wet Tundra		Canada	N 48.5	W 58.5	0.1	4.5	2015-6 to 2016-9	Gong et al. (2019)
B1	Boreal Forest		Russia	N 64.5	E 100	1.4	5.8	2005-6 to 2007-9	Morishita et al. (2014)
B2	Boreal Forest	Joensuu, Eastern Finland	Finland	N 62.5	E 29.5	1.6	4.3	2007-3 to 2007-9	Maljanen et al. (2010)
B3	Boreal Forest	New Hampshire	USA	N 44.0	W 72	1.3	3.9	1997-12 to 2000-4	Groffman et al. (2006)
B4	Boreal Forest	Daxing'an Mountain	China	N 53.5	E 122.5	1.0	5.6	2016-5 to 2016-12	Wu et al. (2019)
B5	Boreal Forest	Ballyholly	Ireland	N 52.0	W 8.5	1.3	3.4	1993-11 to 1995-7	Butterbach-Bahl et al. (1998)
B6	Boreal Forest	Yakutsk,Eastern Siberia	Russia	N 62.5	E 129.5	1.1	7.9	2004-6 to 2005-9	Takakai et al. (2008)
B7	Boreal Forest	Great Hing'an Mountains	China	N 53	E 123	14.0	4.6	2013-5 to 2015-10	Cui et al. (2018)
B8	Boreal Forest	Mid-boreal Upland Ecoregion of central Saskatchewan	Canada	N 53.5	W 105.5	1.1	5.7	2006-5 to 2007-10	Matson et al.(2009)

https://doi.org/10.5194/egusphere-2023-1047
Preprint. Discussion started: 19 June 2023

B9	Boreal Forest	Mont St. Hilaire	Canada	N 45.6	W 73.2	0.7	4.7	2006-5 to 2008-5	Ullah & Moore (2011)
B10	Boreal Forest	Southern Finland	Finland	N 61.3	E 25	1.2	3.7	2000-6 to 2003-8	Maljanen et al. (2006)
B11	Boreal Forest	Southern Lower Saxony	Germany	N 51.6	E 10.1	1.3	4.5	1999-4 to 2000-3	Teepe et al. (2004)
B12	Boreal Forest	Hoglwald Forest	Germany	N 48.5	E 11.2	1.0	3.6	1995-1 to 1997-12	Luo t al. (2013)
A1	Dry Tundra	Yakutsk, Eastern Siberia	Russia	N 62.3	E 129.5	1.4	8.3	2004-6 to 2005-9	Takakai et al. (2008)
A2	Alpine Tundra	Changbai Mountain	China	N 42.5	E 128.0	0.8	7.3	2011-7 to 2013-9	Zhou et al. (2016)
A3	Alpine Meadow	Qinghai–Tibetan Plateau	China	N 31.4	E 92.0	1.0	5.3	2015-5 to 2016-12	Yan et al. (2018)
A4	Alpine Meadow	Tibetan Plateau	China	N 37.5	E 101.5	0.8	8.4	2013-2014	Du et al.(2016)
A5	Upland Grassland	Daun	German	N 50.2	E 6.8	1.3	5.1	1997-4 to 1998-3	Anger et al. (2003)
A6	Upland Grassland	French Massif Central region	France	N 45.7	E 3.0	1.2	6.2	2007-4 to 2009-3	Cantarel et al. (2011)

The N_2O emission observational data was organized on a monthly basis over the measurement period. Data of soil density and pH were obtained from the same publications or

https://doi.org/10.5194/egusphere-2023-1047
Preprint. Discussion started: 19 June 2023

relevant publications associated with the same site, or from the global soil bulk density map (Global Soil Data Task, 2000) and Global Database of Soil Properties (Carter and Scholes., 2000). Meteorological data including air temperature, water vapor pressure, precipitation, and cloudiness were collected from literature or the Climate Research Unit (CRU TS v. 4.05) (Harris et al. 2020).

We use PEST (V17.2 for Linux) for parameterization (https://pesthomepage.org/) of nitrification and denitrification parameters for major ecosystem types in the region (Table 2). The parameters are obtained through minimizing the difference between simulated and observed N_2O emissions (Figure 2).

Table 2. Parameter values in nitrification and denitrification used in this study (Average ± standard error).

	K1	Kmax	fno3k	fco2k	kn
Boreal Forest	0.2 ± 0.05	0.21 ± 0.07	1.23 ± 0.1	0.08 ± 0.01	0.016 ± 0.001
Wet Tundra	0.19 ± 0.1	0.0003 ± 0.0003	0.62 ± 0.36	0.075 ± 0.02	0.0055 ± 0.005
Alpine Tundra	0.23 ± 0.07	0.13 ± 0.07	0.94 ± 0.16	0.08 ± 0.02	0.012 ± 0.004

https://doi.org/10.5194/egusphere-2023-1047
Preprint. Discussion started: 19 June 2023

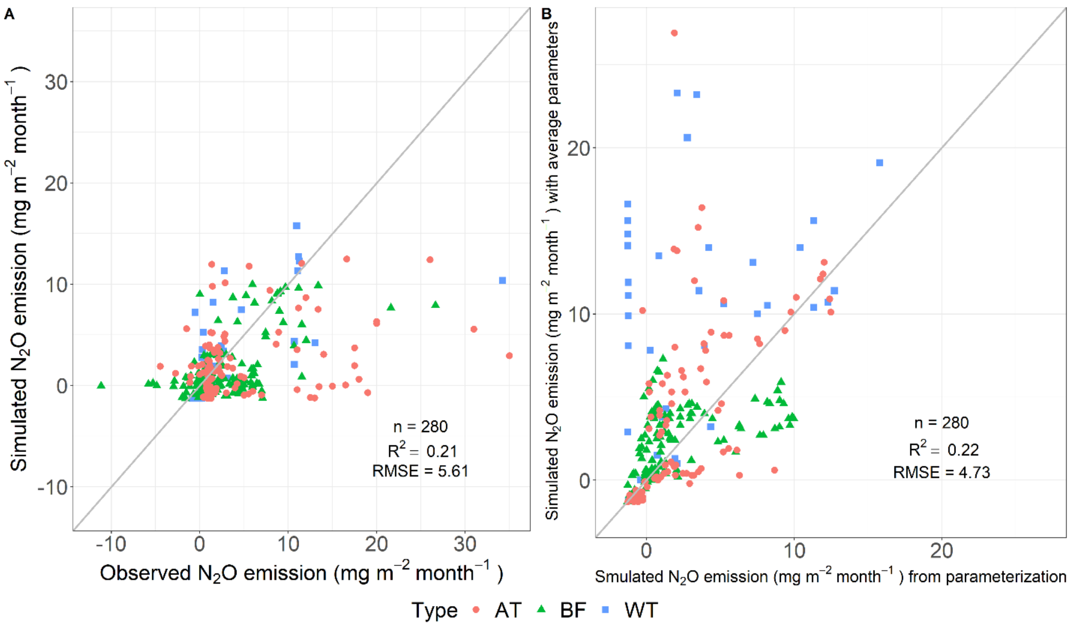

Figure 2. Comparison between the simulated and observed N_2O emissions (A) and simulated N_2O emissions using averaged parameters and simulated N_2O emissions (B) for alpine tundra (AT), boreal forest (BF) and wet tundra (WT). The grey line represents y=x.

2.3 Regional extrapolation

To get the spatially and temporally explicit estimates of N_2O emission at the regional scale, we used the data of land cover, soils, and climate from various sources at a spatial resolution of 0.5° latitude × 0.5° longitude to drive TEM. We used climate forcing data including the monthly CRU TS v. 4.05 data during 1969 –2019. Data of soil density and pH were obtained from the global soil bulk density map (Global Soil Data Task, 2000) and the Global Database of Soil Properties (Carter and Scholes., 2000). The regional N deposition data is sourced from re-gridded model results from GEOS-Chem (Ackerman et al., 2018). We assumed half of the inorganic N deposition is NH_4^+. Gaps between modeled years were filled with the average values between two time periods.

https://doi.org/10.5194/egusphere-2023-1047
Preprint. Discussion started: 19 June 2023

We also conducted model sensitivity test of N_2O emissions, nitrification, and denitrification by increasing or decreasing temperature by 3 °C and increasing or decreasing precipitation by 30% for each gird while keeping all other meteorological input the same, from 1969 to 2019.

3 Results

3.1 Annual emissions of N_2O

TEM estimated that the annual N_2O emissions in pan-Arctic region increased from 1969 to 2019, with the highest value of 1.14 Tg N yr^{-1} in 2011 and the lowest value of 1.09 Tg N yr^{-1} in 1992 without considering the effect of permafrost thawing (hereafter, referred to as base simulation). When permafrost thawing effects were included (hereafter, referred to as permafrost thawing simulation), the emissions were highest in 2019 (1.19 Tg N yr^{-1}) and lowest in 1992 (1.1 Tg N yr^{-1}) (Figure 3). The difference between base simulation and permafrost thawing simulation increases with the largest difference in the last year of our simulation (2019, 4.8%).

https://doi.org/10.5194/egusphere-2023-1047
Preprint. Discussion started: 19 June 2023

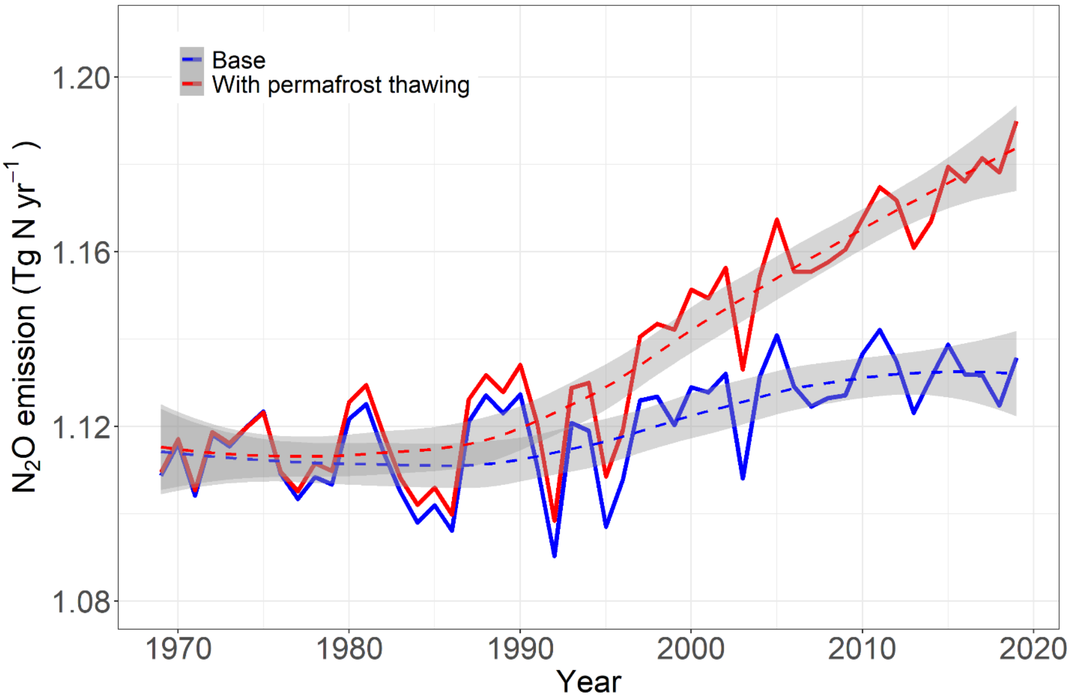

Figure 3. Annual N_2O emissions from pan-Arctic terrestrial ecosystems from 1969 to 2019 in base simulation (blue) and permafrost thawing simulation (red). The dashed curves are locally estimated scatterplot smoothing (LOOSE) lines.

Our calibration provides lower and upper bounds of parameters for each ecosystem type in the pan-arcitc region. Based on these parameter values, our model estimates that regional N_2O emissions range from 0.82 to 0.87 Tg N yr $^{-1}$ and 1.4 to 1.46 Tg N yr $^{-1}$ for the periods of 1969 to 2019 (Appendix A, Figure A1).

3.2 Spatial variability of N_2O emissions

Spatially, in the base simulation, the N_2O emissions range from -12.41 mg N m^{-2} yr^{-1} to 686.02 mg N m^{-2} yr^{-1} in 1969 -1973 period, and from -12.35 mg N m^{-2} yr^{-1} to 686.81 mg N m^{-2} yr^{-1} in 2015 - 2019 period. The ecosystems with net sink of N_2O (N_2O net emission < 0.0) are mainly scattered in higher latitude regions (>65°), while the hotspots for net N_2O sources are

https://doi.org/10.5194/egusphere-2023-1047
Preprint. Discussion started: 19 June 2023

concentrated in the lower latitude regions (<65°) (Figure 4). The general spatial pattern remains relatively stable from 1969 to 2019. However, over this period, the net sink areas of N_2O reduced from 3.08% to 2.54% in the region.

Considering permafrost thawing effects, simulated N_2O emission ranges from -12.41 mg N m^{-2} yr^{-1} to 686.02 mg N m^{-2} yr^{-1} in 1969-1973 period, from -10.59 mg N m^{-2} yr^{-1} to 703.42 mg N m^{-2} yr^{-1} in the 2015-2019 period. Similar to the base simulation, the general spatial pattern does not have an obvious change from 1969 to 2019. However, from 1969 to 2019, the proportion of net sink grid cells of N_2O decreases from 3.07% to 1.95% in the region.

https://doi.org/10.5194/egusphere-2023-1047
Preprint. Discussion started: 19 June 2023

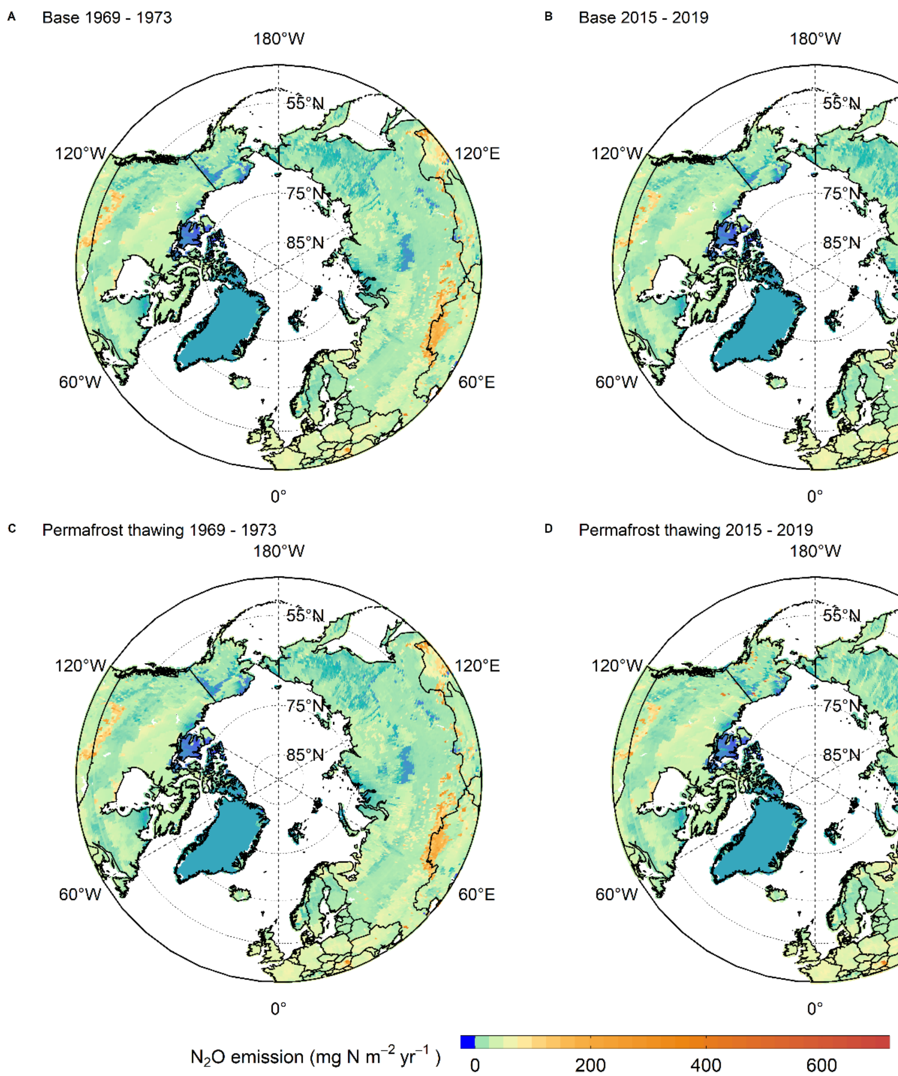

Figure 4. Averaged net annual N_2O emissions in the pan-Arctic from 1969 to 1973 (A) and from 2015 to 2019 (B) of the base simulation and the simulation considering permafrost thawing effects (C and D). Blue indicates the net N_2O sink (negative values).

https://doi.org/10.5194/egusphere-2023-1047
Preprint. Discussion started: 19 June 2023

3.3 Model sensitivity

Table 3. Sensitivity of N_2O emissions, nitrification rate, and denitrification in the pan-Arctic region to changing temperature and precipitation between 1969 and 2019.

	Temperature +3 °C	Temperature -3 °C	Precipitation + 30%	Precipitation - 30%
N_2O emissions (%)	21.2 ± 0.47	-20.9 ± 0.42	2.69 ± 0.53	-2.22 ± 0.5
Nitrification rate (%)	9.4 ± 0.36	-16.6 ± 0.27	-0.24 ± 0.19	-0.73 ± 0.24
Denitrification rate (%)	25.0 ± 0.68	-22.7 ± 0.47	0.55 ± 0.62	0.54 ± 0.41

Model sensitivity analysis shows that summed N_2O emissions are highly sensitive to changes in temperature (± 3 °C) but less sensitive to precipitation change (± 30%). In general, higher temperature and precipitation levels encourage N_2O emissions in the region, while lower temperature and precipitation inhibit the emission. Regional nitrification rate increases by about 10% while denitrification increases about 25% under 3°C temperature increase, leading to an N_2O emission increase by 21% (Table 3). Conversely, decreasing temperature by 3°C results in a similar magnitude decrease of N_2O emissions and denitrification rate, but nitrification tends to decrease more. The total nitrification and denitrification rates exhibit smaller sensitivity to precipitation. Precipitation changes by 30% did not induce dramatic change in both summed nitrification rate and denitrification rate, thus, the regional net N_2O emissions in values. Spatially, pan-Arctic region shows various responses to the changes in precipitation in nitrification and denitrification rates. Nitrification has an optimal value of soil moisture, thus soil moisture differences in the region result in large different emission responses under both higher (+30%) and lower (-30%) precipitation conditions. In addition to the effect of precipitation on soil moisture, denitrification is also influenced by nitrification since nitrification provides substrate NO_3^- for denitrification, leading to variation in denitrification rate at different grid cells

https://doi.org/10.5194/egusphere-2023-1047
Preprint. Discussion started: 19 June 2023

in the region.

4 Discussion

4.1 The role of soil N_2O uptake in net emissions

Wetlands and peatlands are considered as the major N_2O sinks (Schlesinger 2013). Soil water or oxygen content, mineralization, temperature, pH, concentrations of electron donors and acceptors influence soil N_2O uptake (Wen et al., 2016; Chapuis-Lardy et al., 2007). Negative N_2O fluxes were observed at various ecosystem sites in the pan-Arctic (Takakai et al., 2008; Gong et al., 2019; Morishita et al 2014; Groffman et al., 2006; Wu et al., 2019; Butterbach-Bahl et al., 1998; Cui et al., 2018; Matson et al., 2009; Ullah and Moore 2011; Teepe et al., 2004a; Zhou et al., 2016; Cantarel et al., 2011; Goldberg & Gebauer 2009).

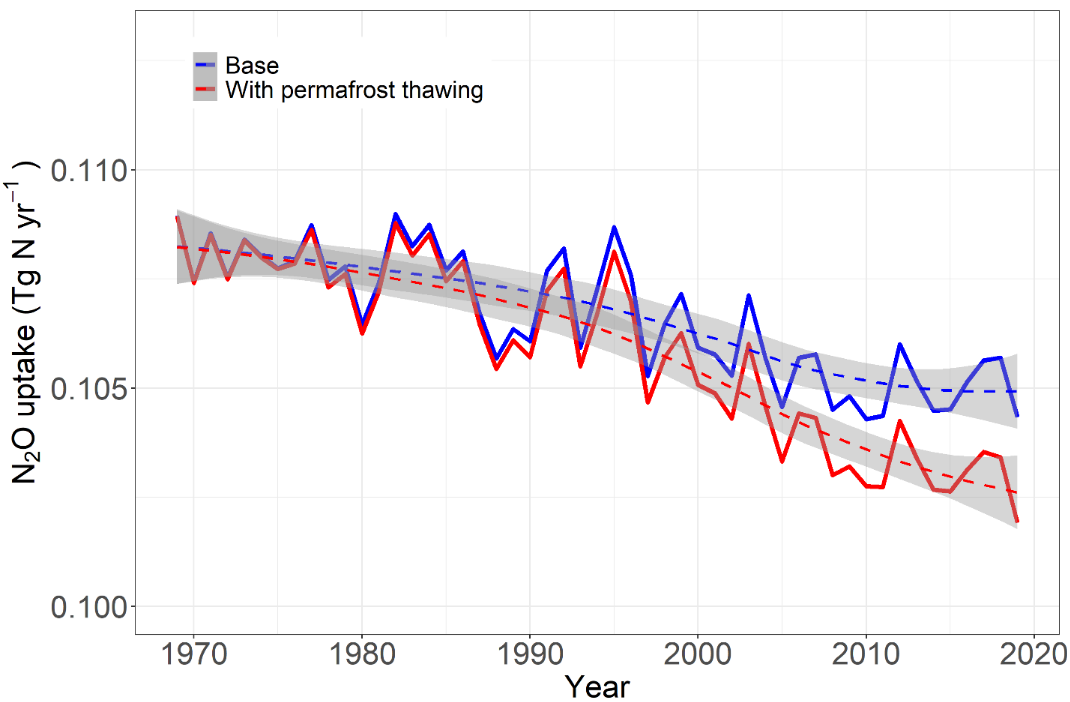

Figure 5. Annual N_2O uptake in pan-Arctic terrestrial ecosystems from 1969 to 2019 in base

https://doi.org/10.5194/egusphere-2023-1047
Preprint. Discussion started: 19 June 2023

(blue) and permafrost thawing simulations (red). The dashed curves are locally estimated scatterplot smoothing (LOOSE) lines.

In our simulation, the total N_2O uptake in pan-Arctic terrestrial ecosystems slightly declines in both base and permafrost thawing simulations (Figure 5) over the simulation period. The highest value of N_2O uptake (0.11 Tg N yr^{-1}) under base simulation was estimated in 1982 and the lowest value of 0.1 Tg N yr^{-1} in 2010, while permafrost simulation has the highest value in 1969 of 0.11 Tg N yr^{-1} and the lowest value in 2019 of 0.1 Tg N yr^{-1}. N_2O uptake accounts for 8.28 - 8.92% of the total production and 9.14 - 9.24% of the total emission in base simulation, 7.8 - 8.86% of total production and 8.57- 9.85% of the total emission in permafrost thawing simulation. N_2O uptake mostly occurs in winter when soils have the lowest production of N_2O with the maximum N_2O uptake reaching 0.05 mg N m^{-2} day^{-1}. Previous study suggests that the median uptake potential is 4 μg N m^{-2} h^{-1} and global consumption is less than 0.3 Tg N yr^{-1} (Schlesinger 2013). The projected sink is about 5% of the currently estimated global net N_2O fluxes from soils to the atmosphere (Schlesinger 2013). N_2O uptake in the pan-Arctic region plays a more significant role than globally.

In our model, the N_2O uptake is calculated based on constant N_2O concentration in the atmosphere. However, the soil released N_2O increases, leading to higher N_2O concentrations in the atmosphere, consequently, increasing the N_2O uptake from the atmosphere. If considering the increasing atmospheric N_2O concentration, the total N_2O uptake amount may be altered. Current simulation only considered the physical process of diffusion because the biochemical processes have not been well understood. However, N_2O is consumed in several reactions of nitrification (Wrage et al., 2004), and under anaerobic conditions, incomplete denitrification produces N_2O whereas the terminal step of denitrification (i.e., the reduction of N_2O to N_2 with the absence of

https://doi.org/10.5194/egusphere-2023-1047
Preprint. Discussion started: 19 June 2023

nosZ gene) consumes N_2O (Wen et al., 2016, Shan et al., 2021). In addition, within the soil profile and in the soil air-filled pores, N_2O can be further reduced to N_2 during its transport to the soil surface (Chapuis-Lardy et al., 2007; Wen et al., 2016, Yang & Silver., 2016). We expect an increase in N_2O uptake by taking these processes into account.

4.2 The role of N deposition in regional N_2O emissions

In field observations, nitrogen deposition has been shown to induce a substantial increase of N_2O emissions of around 95% in dry alpine meadow (Yan et al., 2018), grasslands (Du et al., 2021), boreal and temporal forests (Deng et al., 2020). In our simulation, the impact of N deposition on N_2O emissions varies at different sites depending on initial conditions and the amount of N deposition.

https://doi.org/10.5194/egusphere-2023-1047
Preprint. Discussion started: 19 June 2023

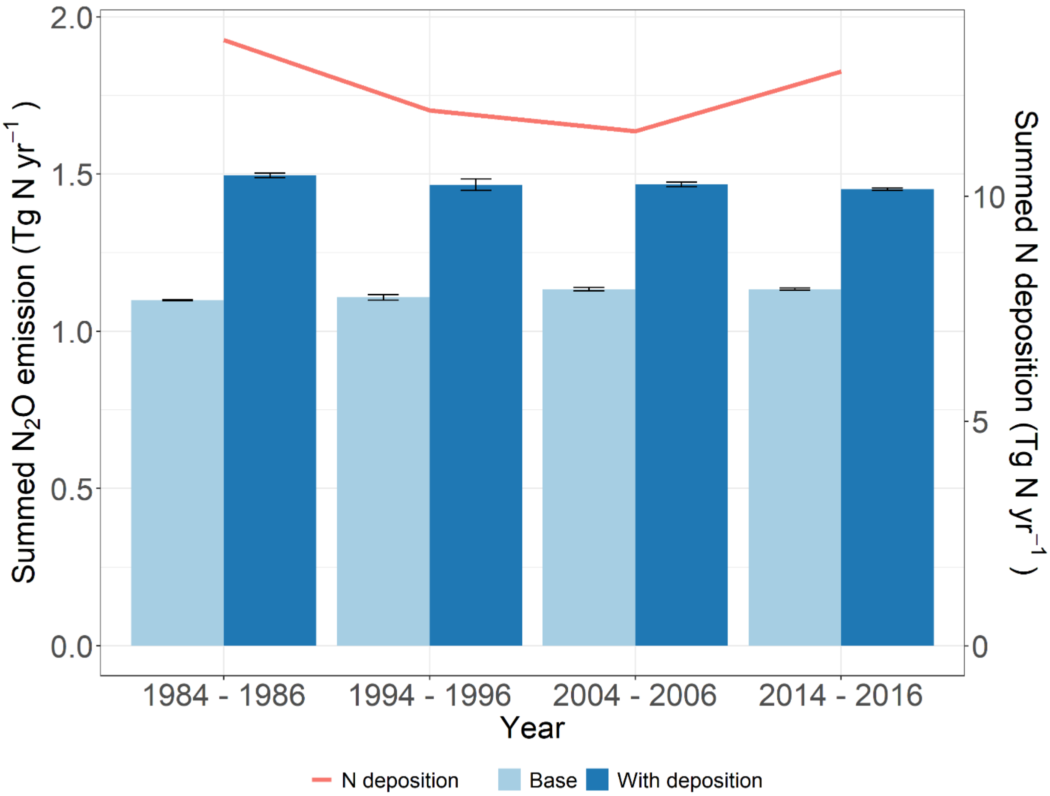

Figure 6. Modeled annual net N_2O emissions from pan-Arctic terrestrial ecosystems from 1984 to 2016 with and without considering N deposition effects. Red line represents the total N deposition in pan-Arctic region.

Our simulation indicates that nitrogen deposition from the atmosphere leads to a significant increase (31.5 ± 3.1 %, $p<0.001$) in the total N_2O emissions compared with the simulation without N deposition (Figure 6). With N deposition from the atmosphere, although the spatial distribution of net N_2O sink and the source remains the same, there are more grid cells in lower latitudes (<60°) that have high N_2O emissions (> 100 mg N m^{-2} yr^{-1}, Figure 7), generally following the spatial pattern of nitrogen deposition (Ackerman et al., 2018).

https://doi.org/10.5194/egusphere-2023-1047
Preprint. Discussion started: 19 June 2023

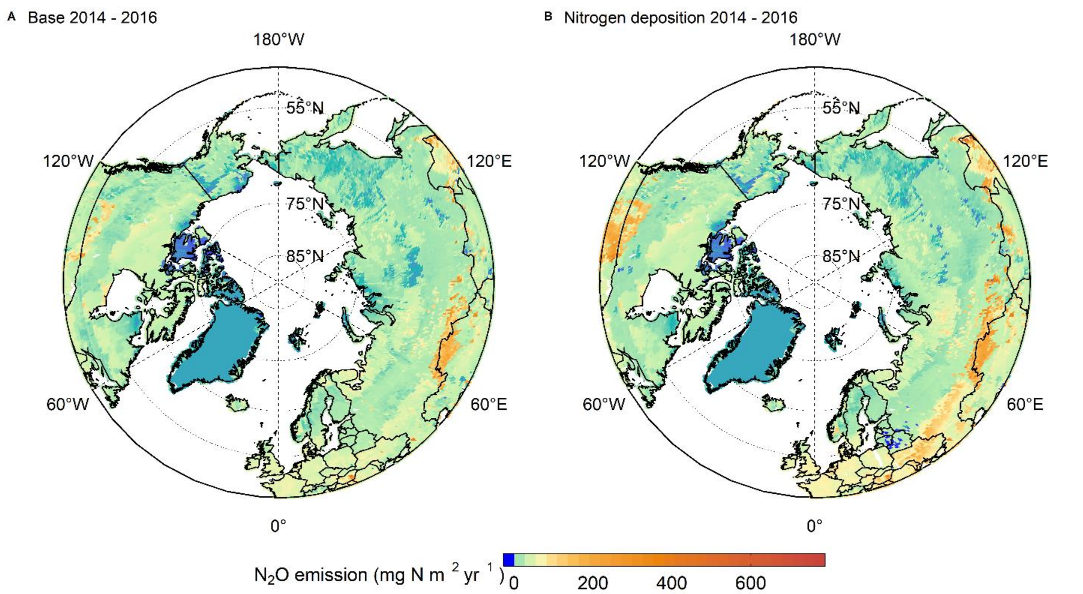

Figure 7. Estimated net N_2O emissions from pan-Arctic terrestrial ecosystems from 2014 to 2016 with (B) and without (A) considering N deposition effects. Blue indicates net sink (negative values).

4.3 The role of permafrost thawing

Permafrost thawing adds more soil organic N for mineralization, consequently, increasing the amount of inorganic N availability, resulting in higher nitrification and denitrification rate (Figure 8A, B, C).

https://doi.org/10.5194/egusphere-2023-1047
Preprint. Discussion started: 19 June 2023

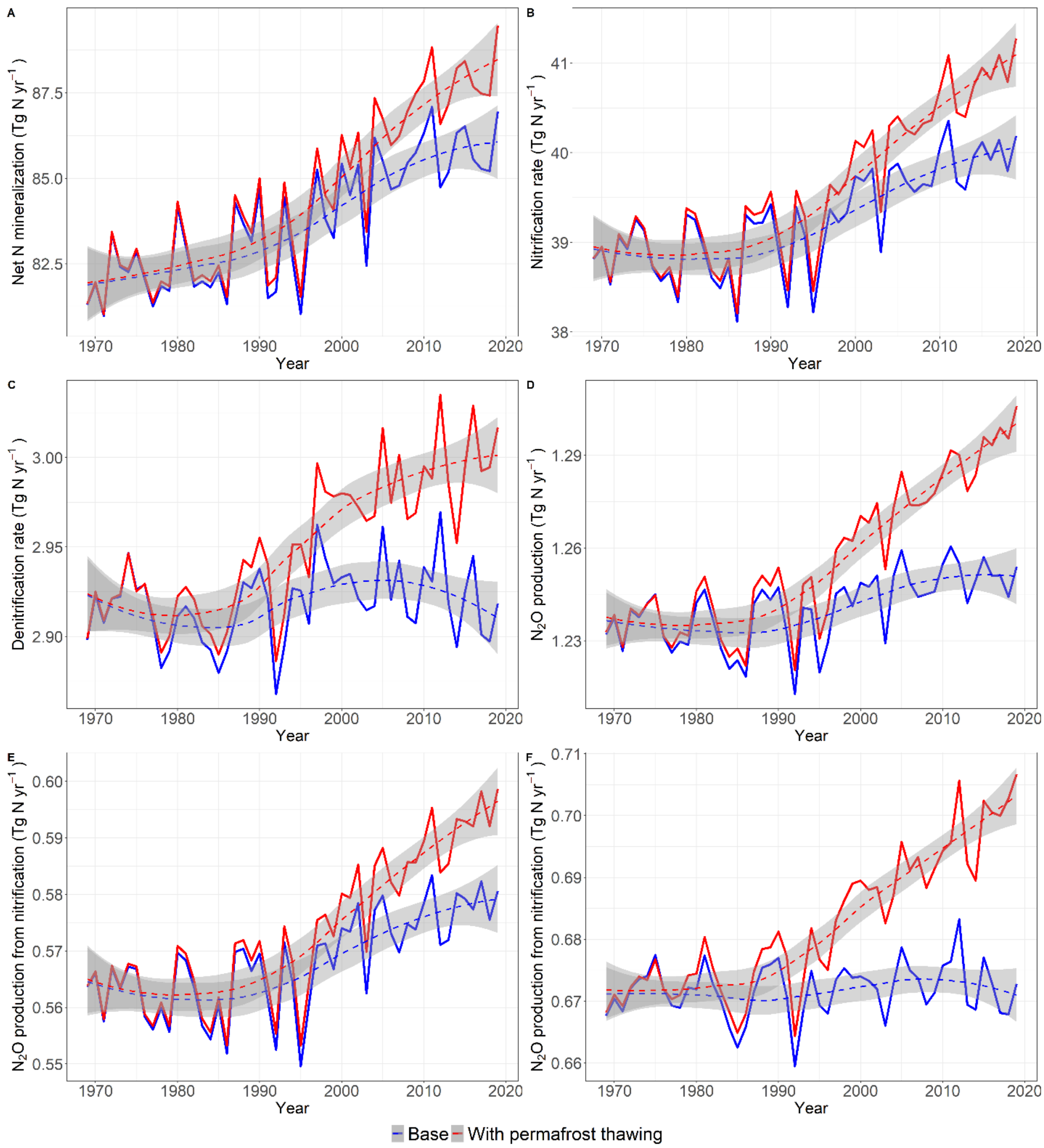

Figure 8. Simulated N mineralization (A), nitrification rate (B), denitrification rate (C), total N_2O production (D), N_2O production from nitrification (E) and N_2O production from denitrification in base (blue) and permafrost thawing simulations (red) from 1969 to 2019. The dashed curves are locally estimated scatterplot smoothing (LOOSE) lines.

In the base simulation, regional nitrification and production of N_2O from nitrification show an upward trend from 1969 to 2019, whereas the denitrification rate slightly decreases and

https://doi.org/10.5194/egusphere-2023-1047
Preprint. Discussion started: 19 June 2023

N_2O production from denitrification remains relatively stable (Figure 5). Higher soil moisture favors denitrification (Klemedtsson et al 1988). Decreasing average soil moisture (Figure A2) may decrease the denitrification rate from 2000 to 2019. In contrast, in the permafrost thawing simulation, the denitrification rate increases from 2000 to 2019. Although lower soil moisture inhibits the denitrification rate, higher nitrification rate provides more NO_3^- for denitrification, making up for the loss caused by lower soil moisture. The higher N_2O production from both nitrification and denitrification contributes to the higher total N_2O production.

Similar to the simulation of the annual N_2O emissions (N_2O production - N_2O uptake) in the pan-Arctic region, the N_2O production generally increased from 1969 to 2019 (Figure 6, D), with the highest value of 1.26 Tg N yr^{-1} in 2011 and the lowest value of 1.21 Tg N yr^{-1} in 1992 in the base simulation, and the highest in 2019 (1.31 Tg N yr^{-1}) and lowest in 1992 (1.22 Tg N yr^{-1}) in the permafrost thawing simulation. The difference of N_2O production between base simulation and permafrost thawing simulation increases, with the largest difference in the last year of our simulation (2019, 4.14%). The averaged maximum permafrost thawing depth in the pan-Arctic region increased 0.2 m in our simulation, meaning the organic nitrogen and carbon stored in the 0.2 m permafrost was released. Average temperature in the pan-Arctic region increases from -4.37 °C to -1.37 °C during 1969 - 2019 according to CRU Ts v. 4.05 data. The increasing thawing depth from 1969 to 2019 is small. However, the Arctic region is predicted to warm up to 5.6–12.4 °C and the permafrost is expected to have 3 meters thawing depth (Schuur et al., 2011) for 47-61% area by 2100, which will significantly intensify N_2O emissions from the region.

4.4 Study limitations

There are several limitations to this study. First, current parameterization is based on a

https://doi.org/10.5194/egusphere-2023-1047
Preprint. Discussion started: 19 June 2023

limited amount of observational data. Obtaining additional observations could provide a more complete understanding of the spatial and temporal variability of key parameters that influence N_2O emissions, such as soil moisture, temperature, and N availability.

Second, the uncertainty of input soil data may overestimate N_2O emissions. Specifically, the input of soil bulk density data has a median bulk density value of 1.39 g cm^{-3}, which differs from our observation sites with the median bulk density of 1.13 g cm^{-3}. Similarly, the input of soil pH data has a median value of 6.04 while the median value at observation sites is 4.9. These differences in bulk density and pH between input data at observation sites may bias our model results.

Third, high N_2O emissions during spring thawing and later fall have been observed. Two sources have been proposed to contribute to the enhanced N_2O emissions upon permafrost thawing, including the physical release of N_2O produced throughout the winter and trapped under frozen surface layers and the emission of newly produced N_2O. While early studies suggested that the physical release of accumulated N_2O from subsurface soil layers was the primary mechanism contributing to spring thaw emissions (Risk et al., 2013), most current studies favor the newly produced N_2O as microorganisms remain active during both periods (Teepe et al., 2004b; Röver et al., 1998, Risk et al., 2013) because the timing and amount of N_2O release during thawing do not correspond to the amount of N_2O trapped in soils (Wagner-Riddle et al., 2008; Furon et al., 2008). These "shoulder season" emissions have not been well modeled as the model requires considering the snow dynamics and soil physical models need to be driven with daily data to capture these final temporal scale dynamics. The time step in current model is not fine enough to account for these freeze-thaw processes. In current modeling, the N_2O

https://doi.org/10.5194/egusphere-2023-1047
Preprint. Discussion started: 19 June 2023

emission mainly happens in the growing season, with N_2O emission in winter being negligible. This may cause an underestimate of annual N_2O emissions.

Fourth, while our model simulates nitrogen mineralization by taking into account soil nitrogen availability and environmental factors; recent studies also suggested that soil carbon to nitrogen (C/N) ratio may also play a role in influencing nitrification (Bengtsson et al., 2003; Elrys et al., 2021). This ratio affects the abundance of ammonia-oxidizing bacteria (AOB) and archaea (AOA) (Xiao et al.,2021) and denitrification (Aulakh et al., 2000; Wang et al., 2023). Denitrification prefers a certain range of C/N ratio (Lee et al., 2019). Missing this stochiometric control factor in our model may introduce uncertainties to our estimates.

Finally, our simulation has not included N loading effects caused by dynamics of groundwater, nearby rivers and wetlands, which may significantly influence soil N availability in soils and enhance N_2O emissions (Zhang et al.,2022). The omission of this factor may have led to an underestimation of N_2O emissions. The increasing level of N loading caused by anthropogenic activities may increase the total N_2O emissions and change their spatial patterns. Further research is needed to investigate the extent to which N loading affects N_2O emissions from the region.

5 Conclusions

We use a process-based biogeochemistry model to quantify the regional N_2O emissions considering the effects of N_2O uptake, thawing permafrost, and N deposition. Our simulations show there is an increasing trend in regional net N_2O emissions from 1969 to 2019, ranging from 1.1 to 1.19 Tg N yr^{-1} considering the permafrost thawing effects. Spatially, annual N_2O emissions

https://doi.org/10.5194/egusphere-2023-1047
Preprint. Discussion started: 19 June 2023

or soil N_2O uptake range from -12 to around 700 mg N m^{-2} yr^{-1}, with the negative values indicating an N_2O sink, exhibiting significant spatial variabilities in both N_2O emissions and soil uptake in this region. Nitrogen deposition from the atmosphere leads to a significant increase (31.49 ± 3.09 %) in the emission. Our results suggest that in the future, the pan-Arctic terrestrial ecosystem might act as an even larger N_2O source with more warming, permafrost thawing, and higher N deposition.

Code and data availability. The TEM codes, outputs, and samples of running directory can be accessed via the Purdue University Research Repository doi:10.4231/KZ5W-DC21

Author contributions. YY was responsible for model revision, model simulation and paper writing. QZ was responsible for project design and paper revision. BZ was responsible for model revision support and paper revision. NS was responsible for project design support and paper revision.

Competing interests. The contact author has declared that neither of the authors has any competing interests.

Financial support. This research has been supported by the National Science Foundation (grant no. 1802832).

https://doi.org/10.5194/egusphere-2023-1047
Preprint. Discussion started: 19 June 2023

Reference

Abbott, B. W. and Jones, J. B.: Permafrost collapse alters soil carbon stocks, respiration, CH_4, and N_2O in upland tundra, Glob Change Biol, 21, 4570–4587, https://doi.org/10.1111/gcb.13069, 2015.

Ackerman, Daniel E; Chen, Xin; Millet, Dylan B: Global nitrogen deposition (2°×2.5° grid resolution) simulated with GEOS-Chem for 1984-1986, 1994-1996, 2004-2006, and 2014-2016, https://doi.org/10.13020/D6KX2R, 2018.

Anger, M., Hoffmann, C., and Kühbauch, W.: Nitrous oxide emissions from artificial urine patches applied to different N-fertilized swards and estimated annual N_2O emissions for differently fertilized pastures in an upland location in Germany, Soil Use and Management, 19, 104–111, https://doi.org/10.1111/j.1475-2743.2003.tb00288.x, 2006.

Aulakh, M. S., Khera, T. S., and Doran, J. W.: Mineralization and denitrification in upland, nearly saturated and flooded subtropical soil, Biology and Fertility of Soils, 31, 168–174, https://doi.org/10.1007/s003740050641, 2000.

Bengtsson, G., Bengtson, P., and Månsson, K. F.: Gross nitrogen mineralization-, immobilization-, and nitrification rates as a function of soil C/N ratio and microbial activity, Soil Biology and Biochemistry, 35, 143–154, https://doi.org/10.1016/S0038-0717(02)00248-1, 2003.

Borge, A. F., Westermann, S., Solheim, I., and Etzelmüller, B.: Strong degradation of palsas and peat plateaus in northern Norway during the last 60 years, The Cryosphere, 11, 1–16, https://doi.org/10.5194/tc-11-1-2017, 2017.

Bose, K. S. and Sarma, R. H.: Delineation of the intimate details of the backbone conformation of pyridine nucleotide coenzymes in aqueous solution, Biochem Biophys Res Commun, 66, 1173–1179, https://doi.org/10.1016/0006-291x(75)90482-9, 1975.

Butterbach-Bahl, K., Gasche, R., Huber, C., Kreutzer, K., and Papen, H.: Impact of N-input by wet deposition on N-trace gas fluxes and CH_4-oxidation in spruce forest ecosystems of the temperate zone in Europe, Atmospheric Environment, 32, 559–564, https://doi.org/10.1016/S1352-2310(97)00234-3, 1998.

Cantarel, A. A. M., Bloor, J. M. G., Deltroy, N., and Soussana, J.-F.: Effects of Climate Change Drivers on Nitrous Oxide Fluxes in an Upland Temperate Grassland, Ecosystems, 14, 223–233, https://doi.org/10.1007/s10021-010-9405-7, 2011.

Carter, A. J. and Scholes, R. J.: SoilData v2.0: Generating a Global Database of Soil Properties CSIR Environmentek, Pretoria, South Africa, 2000.

Chapuis-Lardy, L., Wrage, N., Metay, A., Chotte, J.-L., and Bernoux, M.: Soils, a sink for N_2O? A review, Glob Change Biol, 13, 1–17, https://doi.org/10.1111/j.1365-2486.2006.01280.x, 2007.

https://doi.org/10.5194/egusphere-2023-1047
Preprint. Discussion started: 19 June 2023

Cui, Q., Song, C., Wang, X., Shi, F., Yu, X., and Tan, W.: Effects of warming on N_2O fluxes in a boreal peatland of Permafrost region, Northeast China, Science of The Total Environment, 616–617, 427–434, https://doi.org/10.1016/j.scitotenv.2017.10.246, 2018.

Del Grosso, S. J., Parton, W. J., Mosier, A. R., Ojima, D. S., Kulmala, A. E., and Phongpan, S.: General model for N 2 O and N 2 gas emissions from soils due to dentrification, Global Biogeochem Cycles, 14, 1045–1060, https://doi.org/10.1029/1999GB001225, 2000.

Deng, L., Huang, C., Kim, D., Shangguan, Z., Wang, K., Song, X., and Peng, C.: Soil GHG fluxes are altered by N deposition: New data indicate lower N stimulation of the N_2O flux and greater stimulation of the calculated C pools, Glob Change Biol, 26, 2613–2629, https://doi.org/10.1111/gcb.14970, 2020.

Dentener, F., Drevet, J., Lamarque, J. F., Bey, I., Eickhout, B., Fiore, A. M., Hauglustaine, D., Horowitz, L. W., Krol, M., Kulshrestha, U. C., Lawrence, M., Galy-Lacaux, C., Rast, S., Shindell, D., Stevenson, D., Van Noije, T., Atherton, C., Bell, N., Bergman, D., Butler, T., Cofala, J., Collins, B., Doherty, R., Ellingsen, K., Galloway, J., Gauss, M., Montanaro, V., Müller, J. F., Pitari, G., Rodriguez, J., Sanderson, M., Solmon, F., Strahan, S., Schultz, M., Sudo, K., Szopa, S., and Wild, O.: Nitrogen and sulfur deposition on regional and global scales: A multimodel evaluation, Global Biogeochem. Cycles, 20, n/a-n/a, https://doi.org/10.1029/2005GB002672, 2006.

Du, Y., Guo, X., Cao, G., Wang, B., Pan, G., and Liu, D. L.: Simulation and prediction of nitrous oxide emission by the water and nitrogen management model on the Tibetan plateau, Biochemical Systematics and Ecology, 65, 49–56, https://doi.org/10.1016/j.bse.2016.02.002, 2016.

Du, Y., Ke, X., Li, J., Wang, Y., Cao, G., Guo, X., and Chen, K.: Nitrogen deposition increases global grassland N_2O emission rates steeply: A meta-analysis, CATENA, 199, 105105, https://doi.org/10.1016/j.catena.2020.105105, 2021.

Elberling, B., Christiansen, H. H., and Hansen, B. U.: Erratum: High nitrous oxide production from thawing permafrost, Nature Geosci, 3, 506–506, https://doi.org/10.1038/ngeo893, 2010.

Elrys, A. S., Wang, J., Metwally, M. A. S., Cheng, Y., Zhang, J., Cai, Z., Chang, S. X., and Müller, C.: Global gross nitrification rates are dominantly driven by soil carbon-to-nitrogen stoichiometry and total nitrogen, Glob Change Biol, 27, 6512–6524, https://doi.org/10.1111/gcb.15883, 2021.

Frey, K. E., McClelland, J. W., Holmes, R. M., and Smith, L. C.: Impacts of climate warming and permafrost thaw on the riverine transport of nitrogen and phosphorus to the Kara Sea, J. Geophys. Res., 112, n/a-n/a, https://doi.org/10.1029/2006JG000369, 2007.

Furon, A. C., Wagner-Riddle, C., Smith, C. R., and Warland, J. S.: Wavelet analysis of wintertime and spring thaw CO_2 and N_2O fluxes from agricultural fields, Agricultural and Forest Meteorology, 148, 1305–1317, https://doi.org/10.1016/j.agrformet.2008.03.006, 2008.

https://doi.org/10.5194/egusphere-2023-1047
Preprint. Discussion started: 19 June 2023

GLOBAL SOIL DATA TASK: Global Gridded Surfaces of Selected Soil Characteristics (IGBP-DIS), 218.590182 MB, https://doi.org/10.3334/ORNLDAAC/569, 2000.

Goldberg, S. D. and Gebauer, G.: Drought turns a Central European Norway spruce forest soil from an N_2O source to a transient N_2O sink, Glob Change Biol, 15, 850–860, https://doi.org/10.1111/j.1365-2486.2008.01752.x, 2009.

Gong, Y., Wu, J., Vogt, J., and Le, T. B.: Warming reduces the increase in N_2O emission under nitrogen fertilization in a boreal peatland, Science of The Total Environment, 664, 72–78, https://doi.org/10.1016/j.scitotenv.2019.02.012, 2019.

Groffman, P. M., Hardy, J. P., Driscoll, C. T., and Fahey, T. J.: Snow depth, soil freezing, and fluxes of carbon dioxide, nitrous oxide and methane in a northern hardwood forest: SOIL FREEZING AND TRACE GASES, Glob Change Biol, 12, 1748–1760, https://doi.org/10.1111/j.1365-2486.2006.01194.x, 2006.

Grosse, G., Goetz, S., McGuire, A. D., Romanovsky, V. E., and Schuur, E. A. G.: Changing permafrost in a warming world and feedbacks to the Earth system, Environ. Res. Lett., 11, 040201, https://doi.org/10.1088/1748-9326/11/4/040201, 2016.

Harden, J. W., Koven, C. D., Ping, C.-L., Hugelius, G., David McGuire, A., Camill, P., Jorgenson, T., Kuhry, P., Michaelson, G. J., O'Donnell, J. A., Schuur, E. A. G., Tarnocai, C., Johnson, K., and Grosse, G.: Field information links permafrost carbon to physical vulnerabilities of thawing, Geophys. Res. Lett., 39, https://doi.org/10.1029/2012GL051958, 2012.

Harris, I., Osborn, T. J., Jones, P., and Lister, D.: Version 4 of the CRU TS monthly high-resolution gridded multivariate climate dataset, Sci Data, 7, 109, https://doi.org/10.1038/s41597-020-0453-3, 2020.

IPCC (2013), Climate change 2013: The physical science basis. Contribution of working group I to the fifth assessment report of the intergovernmental panel on climate change, edited by T. F. Stocker et al., 1535 pp., Cambridge University. Press, Cambridge, U. K., and New York. https://www.ipcc.ch/report/ar5/wg1/

Jones, B. M., Baughman, C. A., Romanovsky, V. E., Parsekian, A. D., Babcock, E. L., Stephani, E., Jones, M. C., Grosse, G., and Berg, E. E.: Presence of rapidly degrading permafrost plateaus in south-central Alaska, The Cryosphere, 10, 2673–2692, https://doi.org/10.5194/tc-10-2673-2016, 2016.

Klemedtsson, L., Svensson, B. H., and Rosswall, T.: Relationships between soil moisture content and nitrous oxide production during nitrification and denitrification, Biol Fert Soils, 6, https://doi.org/10.1007/BF00257658, 1988.

Kunhikrishnan, A., Thangarajan, R., Bolan, N. S., Xu, Y., Mandal, S., Gleeson, D. B., Seshadri, B., Zaman, M., Barton, L., Tang, C., Luo, J., Dalal, R., Ding, W., Kirkham, M. B., and Naidu, R.: Functional Relationships of Soil Acidification, Liming, and Greenhouse Gas Flux, in:

https://doi.org/10.5194/egusphere-2023-1047
Preprint. Discussion started: 19 June 2023

Advances in Agronomy, vol. 139, Elsevier, 1–71, https://doi.org/10.1016/bs.agron.2016.05.001, 2016.

Lee, Y.-Y., Choi, H., and Cho, K.-S.: Effects of carbon source, C/N ratio, nitrate, temperature, and pH on N_2O emission and functional denitrifying genes during heterotrophic denitrification, Journal of Environmental Science and Health, Part A, 54, 16–29, https://doi.org/10.1080/10934529.2018.1503903, 2019.

Li, C., Frolking, S., and Frolking, T. A.: A model of nitrous oxide evolution from soil driven by rainfall events: 2. Model applications, J. Geophys. Res., 97, 9777–9783, https://doi.org/10.1029/92JD00510, 1992.

Liu, L., Zhuang, Q., Zhao, D., Zheng, D., Kou, D., and Yang, Y.: Permafrost Degradation Diminishes Terrestrial Ecosystem Carbon Sequestration Capacity on the Qinghai-Tibetan Plateau, Global Biogeochem. Cycles, 36, https://doi.org/10.1029/2021GB007068, 2022.

Liu, X., Zhang, Q., Li, S., Zhang, L., and Ren, J.: Simulated NH_4^+-N Deposition Inhibits CH_4 Uptake and Promotes N_2O Emission in the Meadow Steppe of Inner Mongolia, China, Pedosphere, 27, 306–317, https://doi.org/10.1016/S1002-0160(17)60318-7, 2017.

Ludwig, B., Teepe, R., Lopes De Gerenyu, V., and Flessa, H.: CO_2 and N_2O emissions from gleyic soils in the Russian tundra and a German forest during freeze–thaw periods—a microcosm study, Soil Biology and Biochemistry, 38, 3516–3519, https://doi.org/10.1016/j.soilbio.2006.06.006, 2006.

Luo, G. J., Kiese, R., Wolf, B., and Butterbach-Bahl, K.: Effects of soil temperature and moisture on methane uptake and nitrous oxide emissions across three different ecosystem types, Biogeosciences, 10, 3205–3219, https://doi.org/10.5194/bg-10-3205-2013, 2013.

Ma, W. K., Schautz, A., Fishback, L.-A. E., Bedard-Haughn, A., Farrell, R. E., and Siciliano, S. D.: Assessing the potential of ammonia oxidizing bacteria to produce nitrous oxide in soils of a high arctic lowland ecosystem on Devon Island, Canada, Soil Biology and Biochemistry, 39, 2001–2013, https://doi.org/10.1016/j.soilbio.2007.03.001, 2007.

Maljanen, M., Jokinen, H., Saari, A., Strommer, R., and Martikainen, P. J.: Methane and nitrous oxide fluxes, and carbon dioxide production in boreal forest soil fertilized with wood ash and nitrogen, Soil Use & Management, 22, 151–157, https://doi.org/10.1111/j.1475-2743.2006.00029.x, 2006.

Maljanen, M., Alm, J., Martikainen, P. J., and Repo, T.: Prolongation of soil frost resulting from reduced snow cover increases nitrous oxide emissions from boreal forest soil, Boreal Environment Research, 15, 2010.

Martikainen, P. J., Nykänen, H., Crill, P., and Silvola, J.: Effect of a lowered water table on nitrous oxide fluxes from northern peatlands, Nature, 366, 51–53, https://doi.org/10.1038/366051a0, 1993.

https://doi.org/10.5194/egusphere-2023-1047
Preprint. Discussion started: 19 June 2023

Marushchak, M. E., Pitkämäki, A., Koponen, H., Biasi, C., Seppälä, M., and Martikainen, P. J.: Hot spots for nitrous oxide emissions found in different types of permafrost peatlands, Glob Change Biol, 17, 2601–2614, https://doi.org/10.1111/j.1365-2486.2011.02442.x, 2011.

Matson, A., Pennock, D., and Bedard-Haughn, A.: Methane and nitrous oxide emissions from mature forest stands in the boreal forest, Saskatchewan, Canada, Forest Ecology and Management, 258, 1073–1083, https://doi.org/10.1016/j.foreco.2009.05.034, 2009.

McClelland, J. W., Stieglitz, M., Pan, F., Holmes, R. M., and Peterson, B. J.: Recent changes in nitrate and dissolved organic carbon export from the upper Kuparuk River, North Slope, Alaska, J. Geophys. Res., 112, n/a-n/a, https://doi.org/10.1029/2006JG000371, 2007.

Melillo, J. M., McGuire, A. D., Kicklighter, D. W., Moore, B., Vorosmarty, C. J., and Schloss, A. L.: Global climate change and terrestrial net primary production, Nature, 363, 234–240, https://doi.org/10.1038/363234a0, 1993.

Mishra, U., Hugelius, G., Shelef, E., Yang, Y., Strauss, J., Lupachev, A., Harden, J. W., Jastrow, J. D., Ping, C.-L., Riley, W. J., Schuur, E. A. G., Matamala, R., Siewert, M., Nave, L. E., Koven, C. D., Fuchs, M., Palmtag, J., Kuhry, P., Treat, C. C., Zubrzycki, S., Hoffman, F. M., Elberling, B., Camill, P., Veremeeva, A., and Orr, A.: Spatial heterogeneity and environmental predictors of permafrost region soil organic carbon stocks, Sci. Adv., 7, eaaz5236, https://doi.org/10.1126/sciadv.aaz5236, 2021.

Morishita, T., Matsuura, Y., Kajimoto, T., Osawa, A., Zyryanova, O. A., and Prokushkin, A. S.: CH_4 and N_2O dynamics of a Larix gmelinii forest in a continuous permafrost region of central Siberia during the growing season, Polar Science, 8, 156–165, https://doi.org/10.1016/j.polar.2014.01.004, 2014.

Overland, J. E., Wang, M., Walsh, J. E., and Stroeve, J. C.: Future Arctic climate changes: Adaptation and mitigation time scales, Earth's Future, 2, 68–74, https://doi.org/10.1002/2013EF000162, 2014.

Parton, W. J., Mosier, A. R., Ojima, D. S., Valentine, D. W., Schimel, D. S., Weier, K., and Kulmala, A. E.: Generalized model for N_2 and N_2O production from nitrification and denitrification, Global Biogeochem. Cycles, 10, 401–412, https://doi.org/10.1029/96GB01455, 1996.

Post, W. M., Pastor, J., Zinke, P. J., and Stangenberger, A. G.: Global patterns of soil nitrogen storage, Nature, 317, 613–616, https://doi.org/10.1038/317613a0, 1985.

Potter, C. S., Matson, P. A., Vitousek, P. M., and Davidson, E. A.: Process modeling of controls on nitrogen trace gas emissions from soils worldwide, J. Geophys. Res., 101, 1361–1377, https://doi.org/10.1029/95JD02028, 1996.

Qin, Z., Zhuang, Q., and Zhu, X.: Carbon and nitrogen dynamics in bioenergy ecosystems: 1. Model development, validation and sensitivity analysis, GCB Bioenergy, 6, 740–755, https://doi.org/10.1111/gcbb.12107, 2014.

https://doi.org/10.5194/egusphere-2023-1047
Preprint. Discussion started: 19 June 2023

Qin, Z., Zhuang, Q., and Zhu, X.: Carbon and nitrogen dynamics in bioenergy ecosystems: 2. Potential greenhouse gas emissions and global warming intensity in the conterminous United States, GCB Bioenergy, 7, 25–39, https://doi.org/10.1111/gcbb.12106, 2015.

Ravishankara, A. R., Daniel, J. S., and Portmann, R. W.: Nitrous Oxide (N_2O): The Dominant Ozone-Depleting Substance Emitted in the 21st Century, Science, 326, 123–125, https://doi.org/10.1126/science.1176985, 2009.

Repo, M. E., Susiluoto, S., Lind, S. E., Jokinen, S., Elsakov, V., Biasi, C., Virtanen, T., and Martikainen, P. J.: Large N_2O emissions from cryoturbated peat soil in tundra, Nature Geosci, 2, 189–192, https://doi.org/10.1038/ngeo434, 2009.

Risk, N., Snider, D., and Wagner-Riddle, C.: Mechanisms leading to enhanced soil nitrous oxide fluxes induced by freeze–thaw cycles, Can. J. Soil. Sci., 93, 401–414, https://doi.org/10.4141/cjss2012-071, 2013.

Romanovsky, V. E., Smith, S. L., and Christiansen, H. H.: Permafrost thermal state in the polar Northern Hemisphere during the international polar year 2007-2009: a synthesis, Permafrost Periglac. Process., 21, 106–116, https://doi.org/10.1002/ppp.689, 2010.

Röver, M., Heinemeyer, O., and Kaiser, E.-A.: Microbial induced nitrous oxide emissions from an arable soil during winter, Soil Biology and Biochemistry, 30, 1859–1865, https://doi.org/10.1016/S0038-0717(98)00080-7, 1998.

Saikawa, E., Schlosser, C. A., and Prinn, R. G.: Global modeling of soil nitrous oxide emissions from natural processes, Global Biogeochem. Cycles, 27, 972–989, https://doi.org/10.1002/gbc.20087, 2013.

Schlesinger, W. H.: An estimate of the global sink for nitrous oxide in soils, Glob Change Biol, 19, 2929–2931, https://doi.org/10.1111/gcb.12239, 2013.

Schuur, E. A. G. and Abbott, B.: High risk of permafrost thaw, Nature, 480, 32–33, https://doi.org/10.1038/480032a, 2011.

Shan, J., Sanford, R. A., Chee-Sanford, J., Ooi, S. K., Löffler, F. E., Konstantinidis, K. T., and Yang, W. H.: Beyond denitrification: The role of microbial diversity in controlling nitrous oxide reduction and soil nitrous oxide emissions, Glob Change Biol, 27, 2669–2683, https://doi.org/10.1111/gcb.15545, 2021.

Sierra, C. A., Trumbore, S. E., Davidson, E. A., Vicca, S., and Janssens, I.: Sensitivity of decomposition rates of soil organic matter with respect to simultaneous changes in temperature and moisture, J. Adv. Model. Earth Syst., 7, 335–356, https://doi.org/10.1002/2014MS000358, 2015.

Smith, K. A., Thomson, P. E., Clayton, H., Mctaggart, I. P., and Conen, F.: Effects of temperature, water content and nitrogen fertilisation on emissions of nitrous oxide by soils, Atmospheric Environment, 32, 3301–3309, https://doi.org/10.1016/S1352-2310(97)00492-5, 1998.

https://doi.org/10.5194/egusphere-2023-1047
Preprint. Discussion started: 19 June 2023

Strauss, J., Biasi, C., Sanders, T., Abbott, B. W., Von Deimling, T. S., Voigt, C., Winkel, M., Marushchak, M. E., Kou, D., Fuchs, M., Horn, M. A., Jongejans, L. L., Liebner, S., Nitzbon, J., Schirrmeister, L., Walter Anthony, K., Yang, Y., Zubrzycki, S., Laboor, S., Treat, C., and Grosse, G.: A globally relevant stock of soil nitrogen in the Yedoma permafrost domain, Nat Commun, 13, 6074, https://doi.org/10.1038/s41467-022-33794-9, 2022.

Takakai, F., Desyatkin, A. R., Lopez, C. M. L., Fedorov, A. N., Desyatkin, R. V., and Hatano, R.: CH_4 and N_2O emissions from a forest-alas ecosystem in the permafrost taiga forest region, eastern Siberia, Russia, J. Geophys. Res., 113, n/a-n/a, https://doi.org/10.1029/2007JG000521, 2008.

Teepe, R., Vor, A., Beese, F., and Ludwig, B.: Emissions of N_2O from soils during cycles of freezing and thawing and the effects of soil water, texture and duration of freezing: N_2O emissions in freeze-thaw cycles of soils, European Journal of Soil Science, 55, 357–365, https://doi.org/10.1111/j.1365-2389.2004.00602.x, 2004a.

Teepe, R., Brumme, R., Beese, F., and Ludwig, B.: Nitrous Oxide Emission and Methane Consumption Following Compaction of Forest Soils, Soil Sci. Soc. Am. J., 68, 605–611, https://doi.org/10.2136/sssaj2004.6050, 2004b.

Ullah, S. and Moore, T. R.: Biogeochemical controls on methane, nitrous oxide, and carbon dioxide fluxes from deciduous forest soils in eastern Canada, J. Geophys. Res., 116, G03010, https://doi.org/10.1029/2010JG001525, 2011.

Van Bochove, E., Bertrand, N., and Caron, J.: In Situ Estimation of the Gaseous Nitrous Oxide Diffusion Coefficient in a Sandy Loam Soil, Soil Science Society of America Journal, 62, 1178–1184, https://doi.org/10.2136/sssaj1998.03615995006200050004x, 1998.

Voigt, C., Lamprecht, R. E., Marushchak, M. E., Lind, S. E., Novakovskiy, A., Aurela, M., Martikainen, P. J., and Biasi, C.: Warming of subarctic tundra increases emissions of all three important greenhouse gases - carbon dioxide, methane, and nitrous oxide, Glob Change Biol, 23, 3121–3138, https://doi.org/10.1111/gcb.13563, 2017.

Wagena, M. B., Bock, E. M., Sommerlot, A. R., Fuka, D. R., and Easton, Z. M.: Development of a nitrous oxide routine for the SWAT model to assess greenhouse gas emissions from agroecosystems, Environmental Modelling & Software, 89, 131–143, https://doi.org/10.1016/j.envsoft.2016.11.013, 2017.

Wagner-Riddle, C., Hu, Q. C., Van Bochove, E., and Jayasundara, S.: Linking Nitrous Oxide Flux During Spring Thaw to Nitrate Denitrification in the Soil Profile, Soil Sci. Soc. Am. J., 72, 908–916, https://doi.org/10.2136/sssaj2007.0353, 2008.

Wang, J., Huang, Q., Li, Y., Tu, X., Chen, Z., Elrys, A. S., Cheng, Y., and Ma, L.: A shift from nitrification to denitrification-dominated N_2O emission in an acidic soil following organic amendment, Biol Fertil Soils, 59, 117–122, https://doi.org/10.1007/s00374-022-01680-7, 2023.

https://doi.org/10.5194/egusphere-2023-1047
Preprint. Discussion started: 19 June 2023

Wang, T., Yang, D., Yang, Y., Piao, S., Li, X., Cheng, G., and Fu, B.: Permafrost thawing puts the frozen carbon at risk over the Tibetan Plateau, Sci. Adv., 6, eaaz3513, https://doi.org/10.1126/sciadv.aaz3513, 2020.

Wen, Y., Chen, Z., Dannenmann, M., Carminati, A., Willibald, G., Kiese, R., Wolf, B., Veldkamp, E., Butterbach-Bahl, K., and Corre, M. D.: Disentangling gross N_2O production and consumption in soil, Sci Rep, 6, 36517, https://doi.org/10.1038/srep36517, 2016.

Wrage, N., Velthof, G. L., Laanbroek, H. J., and Oenema, O.: Nitrous oxide production in grassland soils: assessing the contribution of nitrifier denitrification, Soil Biology and Biochemistry, 36, 229–236, https://doi.org/10.1016/j.soilbio.2003.09.009, 2004.

Wu, X., Zang, S., Ma, D., Ren, J., Chen, Q., and Dong, X.: Emissions of CO_2, CH_4, and N_2O Fluxes from Forest Soil in Permafrost Region of Daxing'an Mountains, Northeast China, IJERPH, 16, 2999, https://doi.org/10.3390/ijerph16162999, 2019.

Xiao, R., Ran, W., Hu, S., and Guo, H.: The response of ammonia oxidizing archaea and bacteria in relation to heterotrophs under different carbon and nitrogen amendments in two agricultural soils, Applied Soil Ecology, 158, 103812, https://doi.org/10.1016/j.apsoil.2020.103812, 2021.

Yan, Y., Ganjurjav, H., Hu, G., Liang, Y., Li, Y., He, S., Danjiu, L., Yang, J., and Gao, Q.: Nitrogen deposition induced significant increase of N_2O emissions in a dry alpine meadow on the central Qinghai–Tibetan Plateau, Agriculture, Ecosystems & Environment, 265, 45–53, https://doi.org/10.1016/j.agee.2018.05.031, 2018.

Yang, W. H. and Silver, W. L.: Net soil–atmosphere fluxes mask patterns in gross production and consumption of nitrous oxide and methane in a managed ecosystem, Biogeosciences, 13, 1705–1715, https://doi.org/10.5194/bg-13-1705-2016, 2016.

Yang, Z., Ou, Y. H., Xu, X., Zhao, L., Song, M., and Zhou, C.: Effects of permafrost degradation on ecosystems, Acta Ecologica Sinica, 30, 33–39, https://doi.org/10.1016/j.chnaes.2009.12.006, 2010.

Yu, T. and Zhuang, Q.: Quantifying global N_2O emissions from natural ecosystem soils using trait-based biogeochemistry models, Biogeosciences, 16, 207–222, https://doi.org/10.5194/bg-16-207-2019, 2019.

Yu, T. (2016). Quantifying the global N_2O emissions from natural ecosystems using a mechanistically-based biogeochemistry model, MS thesis, http://docs.lib.purdue.edu/dissertations/AAI10145857/

Zhang, Y., Zhang, F., Abalos, D., Luo, Y., Hui, D., Hungate, B. A., García-Palacios, P., Kuzyakov, Y., Olesen, J. E., Jørgensen, U., and Chen, J.: Stimulation of ammonia oxidizer and denitrifier abundances by nitrogen loading: Poor predictability for increased soil N_2O emission, Glob Change Biol, 28, 2158–2168, https://doi.org/10.1111/gcb.16042, 2022.

https://doi.org/10.5194/egusphere-2023-1047
Preprint. Discussion started: 19 June 2023

Zhou, Y., Hagedorn, F., Zhou, C., Jiang, X., Wang, X., and Li, M.-H.: Experimental warming of a mountain tundra increases soil CO_2 effluxes and enhances CH_4 and N_2O uptake at Changbai Mountain, China, Sci Rep, 6, 21108, https://doi.org/10.1038/srep21108, 2016.

Zhuang, Q., Romanovsky, V. E., and McGuire, A. D.: Incorporation of a permafrost model into a large-scale ecosystem model: Evaluation of temporal and spatial scaling issues in simulating soil thermal dynamics, J. Geophys. Res., 106, 33649–33670, https://doi.org/10.1029/2001JD900151, 2001.

Zhuang, Q., McGuire, A. D., Melillo, J. M., Clein, J. S., Dargaville, R. J., Kicklighter, D. W., Myneni, R. B., Dong, J., Romanovsky, V. E., Harden, J., and Hobbie, J. E.: Carbon cycling in extratropical terrestrial ecosystems of the Northern Hemisphere during the 20th century: a modeling analysis of the influences of soil thermal dynamics, Tellus B, 55, 751–776, https://doi.org/10.1034/j.1600-0889.2003.00060.x, 2003.

https://doi.org/10.5194/egusphere-2023-1047
Preprint. Discussion started: 19 June 2023

Appendix A

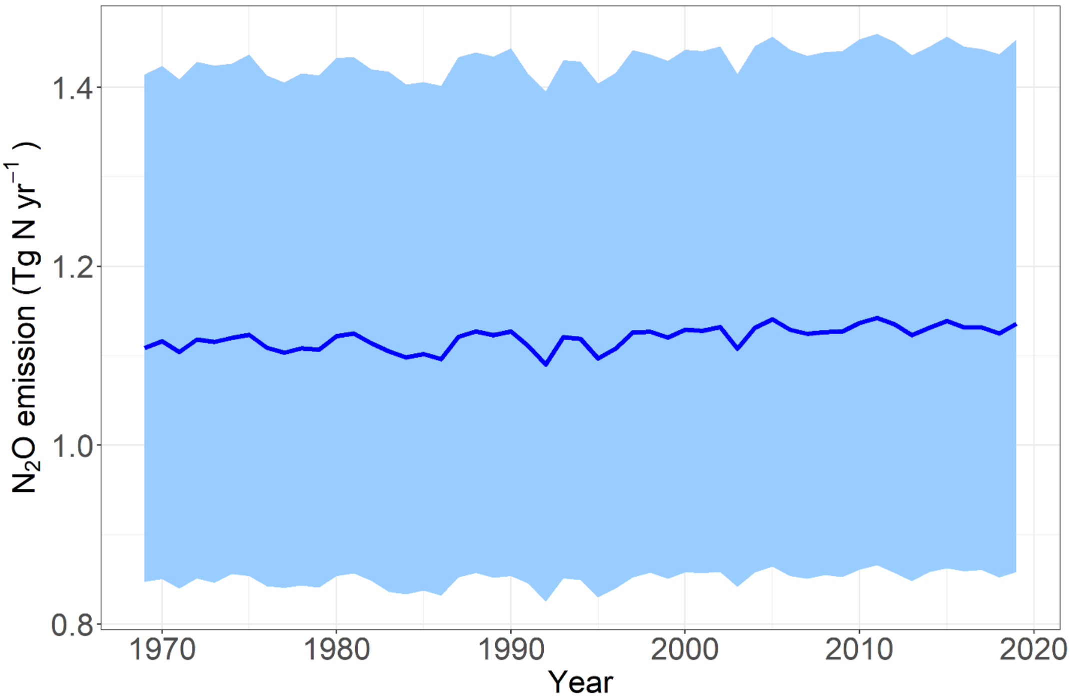

Figure A1. Annual N_2O emissions from pan-Arctic terrestrial ecosystems from 1969 to 2019 in base scenario with boundaries.

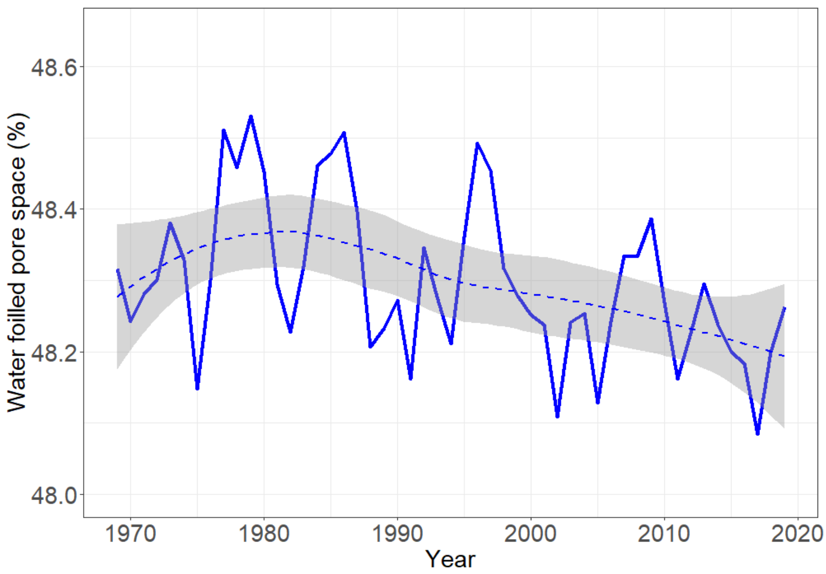

Figure A2. Average soil water filled pore space in the pan-Arctic terrestrial ecosystems from 1969 to 2019.